UNDERSTANDING THE PHYSICAL IMPLICATIONS OF APPROXIMATE ROTOR METHODS USING AN UNSTRUCTURED CFD METHOD

David M. O'Brien, Jr. and Marilyn J. Smith
School of Aerospace Engineering
Georgia Institute of Technology
Atlanta, GA, USA 30332-0150

Abstract

An investigation into the physics of utilizing various rotor approximation techniques on a rotor-fuselage interaction aerodynamics problem has been undertaken. A very simple experimental model consisting of a teetering rotor over a cylinder with a semi-hemispheric nose was chosen for comparison to isolate the basic physical mechanisms. A comparison of actuator disk and actuating blade models with an overset rotor blade model is presented. Methods to implement these models within an unstructured computational code are also described.

Notation

C_P pressure coefficient, $(p-p_\infty)/(0.5r_\infty V_\infty^2)$
C_T thrust coefficient
R rotor radius
V_∞ freestream velocity
β blade flap angle, defined as:
$\beta = \beta_0 + \beta_{1s} \sin\psi + \beta_{1c} \cos\psi$
β_0 coning angle
β_{1c} longitudinal tip path plane tilt angle
β_{1s} lateral tip path plane tilt angle
ψ azimuth angle

Introduction

Rotor-fuselage interaction poses a difficult challenge for computational simulation because of its complex, nonlinear flow field and the difficulties in modeling complex geometries in different reference frames. The need to understand these interactions is necessary if engineers are to obtain reliable performance, vibration and noise predictions for both the rotor and the fuselage. As computers have matured, the techniques utilized to obtain numerical solutions have similarly advanced from momentum theory to vortex-based strategies to higher fidelity Navier-Stokes-based methods. Accounts of the earliest attempts to model main rotor/fuselage interaction are discussed in Landgrebe (Ref. 1) where a comprehensive rotor code was coupled with a fuselage panel method. This research began a trend wherein other researchers (e.g., Refs. 2 and 3) have since applied similar methods with varying success, but the primary drawback with these methods is their inability to model important viscous effects and capture the correct shed vortex structure.

In recent years, researchers have been attempting to simulate more accurate physics for the rotor and fuselage, both individually and in complete rotorcraft models. The intensive development of Computational Fluid Dynamics (CFD) techniques within the fixed-wing community has had a direct benefit in the rotary-wing community. CFD methods have focused on the solution of the steady and unsteady Reynolds-averaged Navier-Stokes (RANS) equations, utilizing a varying fidelity of turbulence modelling to effect closure. Massively parallel computing advances now permit researchers to refine grids to a point where some success has been documented in obtaining accurate loads and a vortex generation and propagation (near-wake). There are three general mesh approaches that have emerged for solving the RANS equations: structured, unstructured and Cartesian. Most codes utilize a structured scheme, since the natural ordering of the nodes reduces the required memory and solution time. However, creating a structured grid can take weeks for very complex configurations. Chimera and/or overset grids can aid in alleviating this problem and success in complex rotorcraft applications is now documented (for example, Refs. 4 and 5). Initial research to apply Cartesian-based structured grid methods is also underway (Ref. 6), though complex configurations still need to be verified using this technique. Unstructured techniques offer the advantage of reduced grid generation times and are easier to adapt to changing configurations. With the recent advances in parallel computing, the increased overhead per node required by unstructured methods is no longer as important an issue, and the additional run time per node is compensated by the grid density optimization. Recent successful publications utilizing unstructured methods in rotor-fuselage interactions include Refs. 5,6, 7, and 8.

These recent rotor-fuselage interaction RANS methods include different fidelities in modeling the rotor. The most physically correct analysis of the rotor-fuselage interaction flow field requires the RANS modeling of the unsteady motion of the rotor blades, as well as a time-accurate analysis of the flow over the fuselage. This is a complex issue since a rotational frame for the rotor and stationary frame for the fuselage must co-exist within the simulation.

Two methods have emerged as potential solutions to the mixed frame problems: overset and/or chimera grids and sliding boundaries. Park and Kwon (Refs. 7 and 8), in Euler simulations, have utilized a rotating cylindrical grid around a main rotor that fits within a rectangular grid about the fuselage and remainder of the control volume. The two grids communicate via a sliding boundary that forms the interface between the two grids. This approach, used in conjunction with unstructured grids, as per Park and Kwon, will minimize the number of grid nodes required to resolve the flow field. The primary drawbacks to this approach are the potential mismatch of flow properties, such as off-body shocks, and the restriction imposed on the type of configurations that can be modeled. Multiple overlapping rotors, such as compound rotors, cannot be modeled. The second approach utilizes a combination of overset and chimera grids to generate smaller grids around each rotor blade, which then rotate through a background Cartesian or unstructured grid. This approach on structured grids was used to correctly capture the general experimental trends on several configurations by Hariharan (Ref. 9), Potsdam et al (Ref. 4 and 5) and Renaud (Ref. 5). This paper will introduce a methodology by which an unstructured overset grid code can be implemented.

The full simulation approach, while the most physically correct, is very CPU and clock time intensive. Many design and analysis needs call for more exact predictions of the fuselage loading, but are content to permit simpler models for the rotor. Several approaches have successfully combined RANS or Euler simulations of the fuselage with simpler rotor models, including a quasi-steady actuator disk (e.g., 10, 11, and 12) and similar unsteady actuator disks have been illustrated by Boyd (Ref. 13), Tadghighi (Ref. 14) and O'Brien (Ref. 12). Both Tadghighi (Ref. 15) and O'Brien (Ref.12) have co-authored papers demonstrating the application of unsteady blade elements as the rotor model.

In all of the preceding publications, different methods of modelling the rotor are discussed and compared in part to experiment and/or other computational methods. There is not, however, a comparison between all of the methods that discusses the physical limitations of each in context to a single configuration. In this study, a steady actuator disk, unsteady actuating blade model, unsteady blade element model, and an overset grid method will be applied on one configuration using an unstructured solver to investigate the different physics captured by each to the rotor-fuselage interaction problem. In addition to the simulation comparisons, the implementation of each model in an unstructured solver is discussed.

Experimental Configuration

Experimentalists at Georgia Tech (GT) have performed a series of studies (Ref. 16) for the aerodynamic interaction between a rotor and a simplified fuselage, as shown in fig. 1. The fuselage consisted of a cylinder with a diameter of 0.134m capped with a hemispherical nose. The fuselage was constructed to be three rotor radii in length (1.3716m). The rotor was a two-bladed, teetering rotor mounted independently of the fuselage using a strut extending from the ceiling. Each rotor blade consisted of a rectangular planform with a constant, untwisted NACA 0015 airfoil section. The blade radius was 0.4572 m with a 2.7% cut out and a chord of 0.086m. The nominal rotation rate for the rotor was 2100 rpm. The hub was located 1 radius downstream of the nose and 0.3 radii above the fuselage centerline. The rotor did not include cyclic pitch as part of an effort to minimize the hub interference. The fuselage strut and rotor shaft sizing were approximated from diagrams in the original test report (Ref. 16).

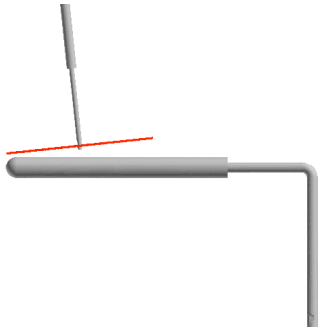

Fig. 1 GT rotor-fuselage test configuration

All computations presented here utilized an advance ratio of 0.1 to maximize the experimental data available and to simulate the large interaction effects between the rotor and the fuselage. To simulate forward flight, the fuselage was aligned with the free stream flow with a rotor shaft tilt of 6 degrees. The blade included a fixed pitch of 10 degrees. The experimental flap angle was measured and an analytical expression determined:

$$\beta = -2.02^\circ \sin\psi - 1.94^\circ \cos\psi \qquad (1)$$

The coning angle was assumed to be zero as the blades have no pre-cone and are rigid. The thrust coefficient (c_T) was measured to be 0.00945, though it should be noted that the lack of cyclic pitch controls prevents the rotor from being trimmed (i.e. the tip path plane is tilted to the side).

Unstructured Methodology: FUN3D

The unstructured methodology utilized to demonstrate the rotor-fuselage interaction is the FUN3D code developed at NASA Langley Research Center (see for example, Ref. 17, 18 and 19). FUN3D solves the Reynolds-Averaged Navier-Stokes (RANS) equations on unstructured tetrahedral meshes in both the compressible and incompressible Mach regimes. The Chorin artificial compressibility method (Ref. 20) is included to model incompressible flows. A first-order backward Euler scheme with local time stepping is applied for steady-state applications, while a second-order backward differentiation formula (BDF) is utilized for time-accurate simulations. A point-implicit relaxation scheme resolves the resulting linearized system. FUN3D stores the flow variables at the vertices of the computation cells and then solves the RANS equations on the non-overlapping control volumes surrounding each node. Roe's flux difference splitting (Ref. 21) calculates the inviscid fluxes on the cell faces, while viscous fluxes are computed with a finite volume formulation so that an equivalent central difference approximation is obtained. While FUN3D has the option of several turbulence models, in this exercise turbulence closure is obtained via the Spalart-Allmaras turbulence model (Ref. 22). The impact of other turbulence models on the GT configuration has been previously discussed in Ref. 23.

Rotor Modeling for Unstructured CFD Methods

As noted in the Introduction section of this paper, most computational methods for rotor-fuselage interaction rely on structured grid implementations. Unstructured meshes have the potential to minimize the computational requirements of these simulations by adding grid refinement only in areas where they are needed. The authors have previously discussed the implementation of actuator disk and blade element models in unstructured methods (see Refs. 12 and 23). For completeness, a short description of these implementations are included here, along with the implementation of an overset unstructured grid system.

Actuator Disk Model

There are two basic methods to implement an actuator disk in any solver, whether it is structured or unstructured. The first approach is based on the momentum/energy source approach proposed by Rajagopalan (Ref. 24). In this approach, source terms modify a) the momentum equations by adding terms to model the force that the rotor blade exerts on the surrounding fluid, and b) the energy equation by adding the work done by the rotor on the fluid. The second approach is to modify the grid so that the rotor disk forms a new boundary condition and the forces and work are added to the RANS equations via an explicit boundary term.

While theoretically both implementations should result in the same simulation, the source approach was found to have a number of advantages over the boundary condition approach, as reported previously by the authors in Ref. 23. The most significant advantage is that the actuator disk surface does not need to be built into the grid, simplifying the grid generation process. One grid can handle an entire parametric study or a trimming procedure. Another advantage is that the source approach was found to be more robust when applied to the incompressible RANS equations. Le Chuiton (Ref. 25) has also concluded that the source approach was superior for modeling compressible flows in structured grids.

The actuator disk is implemented at run time by creating a secondary source grid and associating the sources with the neighboring volume grid nodes. This approach is very similar to an overset approach, but considerably simpler since the source grid represents a permeable surface (i.e. it is not a volume grid) and do not require any type of hole cutting procedure. The forces can be computed prior to run time using constant or linear loadings from simple momentum theory or the results from an external methodology, such as a comprehensive method, as demonstrated in Refs. 5 and 12. Loose coupling can be easily trimmed by using the comprehensive code to develop the trim matrix. Because the grid does not have to be modified as changes in the tip path plane occur, sources can be rapidly updated by changing their strengths and locations. The drawback to this approach is that the source spacing needs to be finer than the local grid spacing or nonphysical solutions can occur (Ref. 23).

Unsteady, Actuating Blade Model

The actuator disk's steady state assumption is not physically realistic when an actual flow induced by a helicopter rotor is assessed. A time-accurate simulation is required to obtain the unsteady characteristics of the flow field. The computational simplicity and efficiency of the actuator disk is appealing, so a concept that can provide both is sought.

An actuating blade model can be simply implemented by utilizing the overset source actuator disk approach and distributing the sources over the actual blade planform as it rotates about the azimuth. This approach can be thought of as a generalization of the unsteady actuator disk models of Boyd (Ref. 13) and Tadghighi (Refs. 14 and 15). The unsteady actuator disk represents a limiting

case of the actuating blade model in which the number of sources along the chord is set to one.

The primary difference between the actuating blade model and the actuator disk model is that the loading is applied in a time-accurate fashion on the actuating blade model. Since the loading is no longer averaged in time, the source positions are moved at each time step by rotating a reference blade at ψ=0° to the appropriate azimuth location. Other blade motions such as lead-lag, flap, and pitch are then applied to refine the position the blade. The final step is to associate the sources with new volume grid nodes.

One difficulty with this model is the determination of the sectional load distribution over the chord. The primary problem was how to correctly load blade sections that existed on multiple partitions. In an effort to simplify the process, each chordwise source used the flow conditions of the nearest grid node to compute the blade loading for section. Each local load was scaled by dividing by the number of sources. As the number of chordwise sources is assigned in advance, the loads are computed independently of one another and avoid the partition problem.

Blade Element Method for Loads

While the actuator blade model improves the solution by adding time-accuracy to the simulation, the computation of the loading is lacking in accuracy. The blade element method adds a more accurate method with which to compute the rotor loading by using two-dimensional airfoil forces and moments based on the local flow conditions. The approach is based on the approach utilized in Zori (Ref. 26) for structured grids. The local flow conditions at each source are set to the flow conditions at the nearest computational grid node. The lift and drag characteristics can be computed using the two-dimensional airfoil characteristics computed from computational techniques, obtained from experimental data, or estimated from thin airfoil theory, similar to the look-up tables (C81 tables) utilized for comprehensive methods.

Overset Rotor Blade Model

The most accurate, and most expensive, method of modelling the rotor for rotor/fuselage interaction is to computationally solve the RANS or Euler equations of motion explicitly. The difficulty in achieving these computations is inherent in the frame of reference that best fits the configurations of the rotor and fuselage. The rotor rotates about an origin typically collocated with the rotor hub, while the fuselage moves with rectilinear motion when level forward flight or hover is modelled. Prior rotor/fuselage simulations of this level of fidelity have utilized overset, structured grids, as in the OVERFLOW code (Ref. 5), or sliding boundaries within unstructured methods (Ref. 8). Each of these has disadvantages, as previously discussed.

Overset grid modelling in FUN3D is achieved using the DiRTlib (Ref. 27) library and SUGGAR (Ref. 28) code. DiRTlib provides the necessary functions to enable the flow solver to utilize overset grids. The only required change to the flow solver is that a set of interface functions be written to work with the library, allowing rapid insertion of overset capabilities. The main function of DiRTlib is to perform the interpolations at the fringes of the component meshes using the domain connectivity information (DCI) generated by a grid assembly program.

SUGGAR is an overset grid assembly program that combines the component meshes into a single composite grid. This is achieved by determining which nodes need to be blanked from the domain and where to interpolate flow information between meshes. SUGGAR writes this information into a DCI file, which is used as input into DiRTlib. For dynamic simulations SUGGAR runs in unison with the flow solver. Once the flow solver completes an iteration, SUGGAR is instructed to generate the new DCI file for the next timestep. When SUGGAR finishes, the flow solver resumes operation and the process continues until the solution converges or a maximum number of iterations is achieved. Rotation about the rotor shaft and the blade flapping motion were included in the present overset simulation.

Results

Two sets of grids were needed for the simulations of the different fidelity rotor disks. Fig. 2 shows a centreline view of the rotor-fuselage grid. The grid consists of a total of 1,449,930 nodes and has 20,335 boundary faces on the fuselage. The surface grid was obtained from a grid independence study for the isolated fuselage configuration. Wind tunnel walls were found not to be a factor in affecting the flow field near the rotor-fuselage. The volume grid was created by concentrating nodes in the region of the rotor wake and near the body. The addition of the overset blade modelling requires additional grids that track the individual blades. Each blade has an additional 420,709 nodes in its overset grid with 15,784 nodes on the surface of the blade. The overset grid is illustrated in fig. 3.

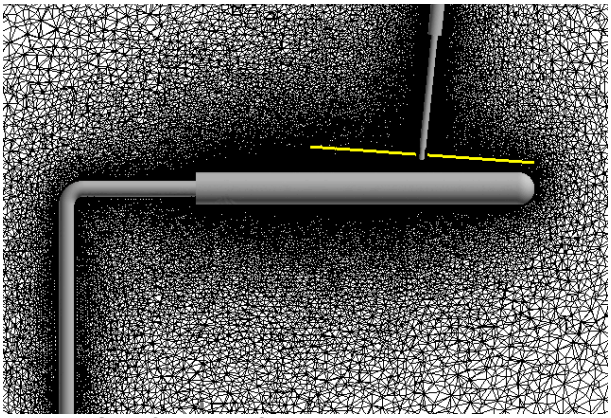

Fig. 2 Grid for simplified rotor models; center plane

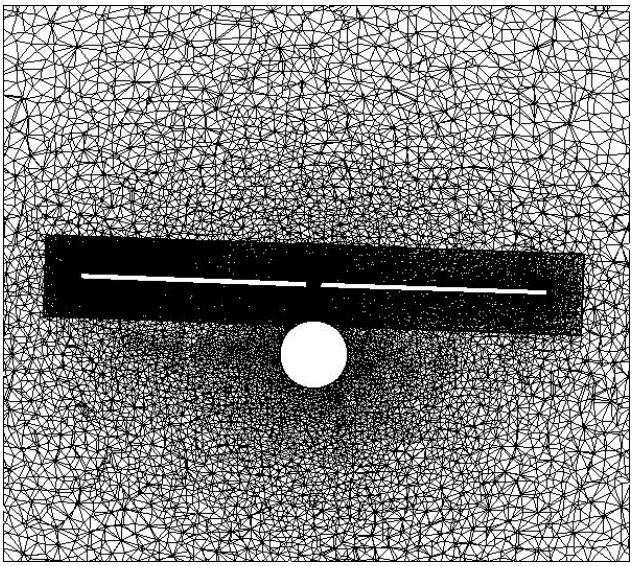

Fig. 3 Overset rotor blade grid

The overset grids include fringe points where each grid independently computes the solution. When the solutions from each grid are overlaid (fig. 4), it is apparent that the solution transitions smoothly across the grid boundaries, as required. Additionally, it is apparent that the solutions are almost identical, notwithstanding the differences in the cell refinement in each grid.

Once the overset methodology was verified to be operating correctly, comparisons of the different methods were undertaken. Flow field and surface features were examined to determine the differences in the physics captured by each rotor method.

Vorticity Isocontours

Vorticity isocontours provide an accurate visual measure of the tip vortex path behind the main rotor. Each of the solutions from the rotor models was plotted using similar scales in fig. 5. The actuator disks show tip vortices shed from the ψ=90^o and 270^o locations. This is not unexpected as the disk acts as a wing and these azimuth locations correspond to the location of the "wing-tips". Also shed from the actuator disk is a vortex sheet corresponding to the trailing edge of the actuator disk. The overall character of the vortical flow does not improve with more accurate load estimation using blade element theory (fig. 5b); the vorticity magnitude appears to change with the change in loading. The advancing side tip vortex is stronger and descends faster than the retreating blade tip vortex with the blade element actuator disk model. As the actuator disk model is steady, these flow fields do not indicate any of the unsteady blade passage vortical features.

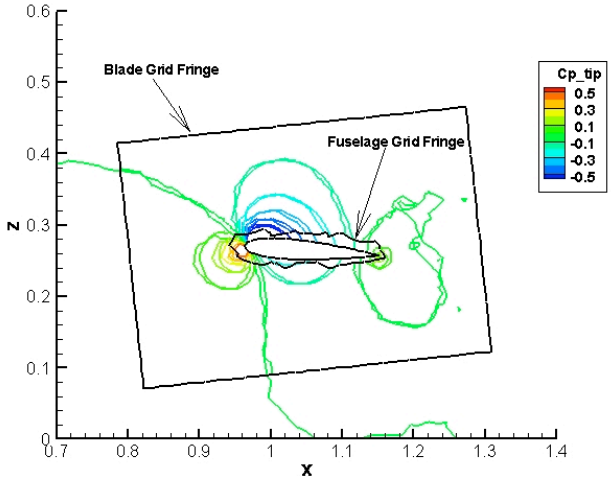

a) Pressure coefficient

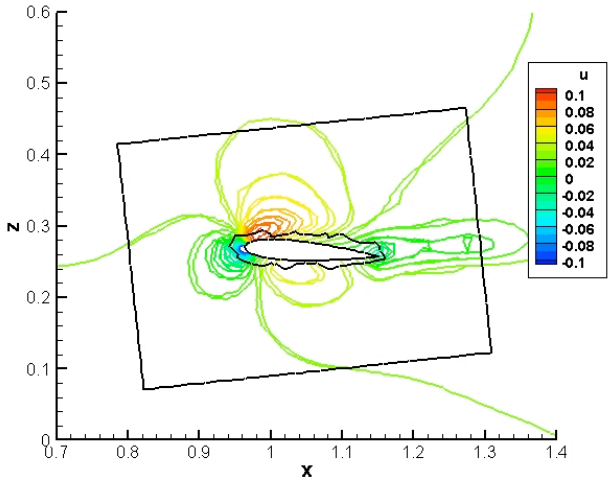

b) u-velocity

Fig. 4 Comparison of the computed solutions in the fuselage and rotor grids using the overset version of FUN3D

With the addition of unsteady actuating blades, the flow field takes on a much different character. The tip vortices can be seen to track with the blades in fig. 5c, and an indication of helix wake structure can be seen aft of the main rotor. It is evident however, that the vortex strength is rapidly dissipating as the isocontours cannot maintain their structure for more than 90° on the retreating side. Vortex-fuselage interaction is observed aft of the main rotor, where the vortex wraps about the fuselage.

The overset blade model provides the most accurate picture (Fig. 5d) of the vorticity shed from the rotor blades. Here, the helical structure of the wake is evident for the entirety of two revolutions simulated. Both the strong tip vortex and weaker root vortices are captured. The interaction of the wake with the fuselage aft of the rotor is more complex; merging of the helical vortices can be seen as the fuselage impedes its downward progress.

Pressure Flowfield

The pressure flow field along the centreline and on the surface is shown in fig. 6 for the converged steady actuator disks and at $\psi=0^{o}$ or $\psi=90^{o}$ for the time-accurate simulations. Identical scales are utilized for ease of comparison between the models. These figures are best utilized in conjunction with the vorticity isocontours of fig. 5 to form an overall view of the flow field.

The constant momentum actuator disk indicates a continuous increase in pressure under most of the rotor disk. A shift in the load distribution from the 180° to the 0° azimuth location corresponds to the tilt of the rotor tip path plane. On the bottom of the fuselage, a very large compression is seen across most of the rotor area. On the side, a suction region appears at approximately 90% of the rotor span and continues to the back edge of the fuselage. Separation at the aft end of the fuselage is also observed.

The blade element actuator disk results in Fig. 6b show differences over the rotor disk that are more physical in nature. The highest suction over the rotor occurs near the blade tips, corresponding to a larger loading on the fuselage beneath these locations. The side suction area has grown significantly, and the aft fuselage shows some pseudo-vortex shedding. No vortex wake-fuselage interaction is seen with either actuator disk formulation.

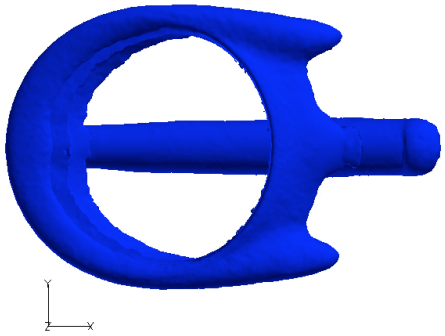

a) Constant Momentum Actuator Disk

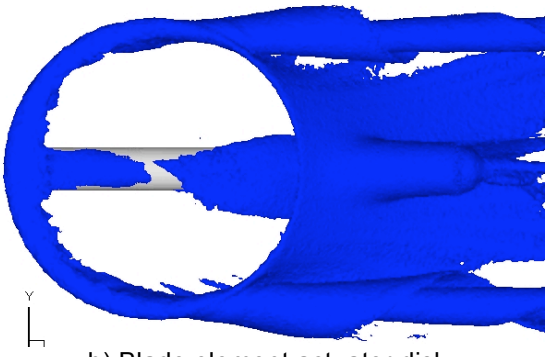

b) Blade element actuator disk

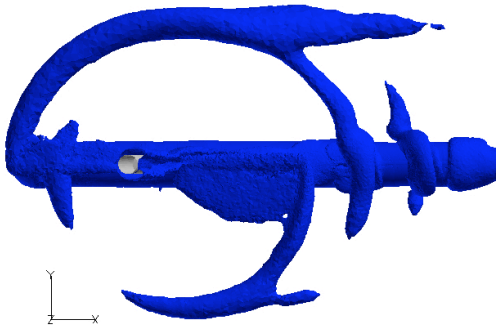

c) Unsteady Actuating Blades

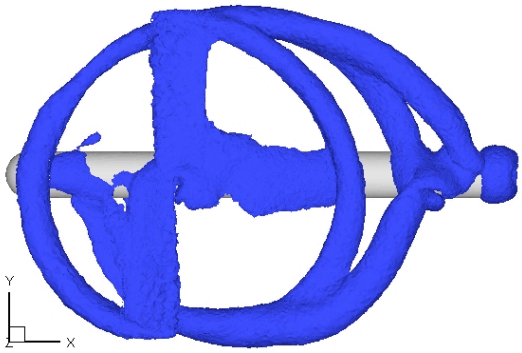

d) Overset Blades

Fig. 5. Vorticity Isocontours

The unsteady actuating blades present similar pressure contours to the actuator disk over the rotor locations. Very large areas of suction above the rotor and download below the rotor are observed. These pressure differentials are larger than those seen in the time-averaged blade element actuator disk. Just aft of the rotor and above the fuselage, the vortex wake can be seen, just as in Fig. 5c. The apparent second interaction between the vortex wake and fuselage, just aft of the first wake, appears to be very weak. The appearance of the wake near the fuselage causes the side suction region to decrease and change shape with the corresponding vortex loading on the fuselage.

The overset blade pressure contours in fig. 6d have a much more discrete character than the first three simulations. There appear to be four separate tip vortex interactions with the fuselage, two from the forward rotor wake and two from the aft rotor wake. Interactions with the root vortex also appear to occur closer to the rotor hub in both the forward and aft portions of the rotor. These appear, as expected, to be weaker in magnitude than the tip vortices. The vortex interactions continue along the sides of the fuselage. The appearance of the discrete vortices indicates that the unsteady interaction for this configuration will be important in computing acoustic and vibration data.

The magnitude of the overset blade download on the fuselage at ψ=0 (see Fig. 7) under the rotor is similar to that predicted by the actuating blades, though the download is greater near the hub region for the overset blades. Aft of the rotor the surface pressures indicate a different suction pattern than the other rotor models. This may be a function of the low number of revolutions utilized for the prediction or that the vortex-fuselage interaction plays a dramatic role in this portion of the fuselage. Further investigation will be needed to clarify this. The pressure distributions located at ψ=90^o indicate that

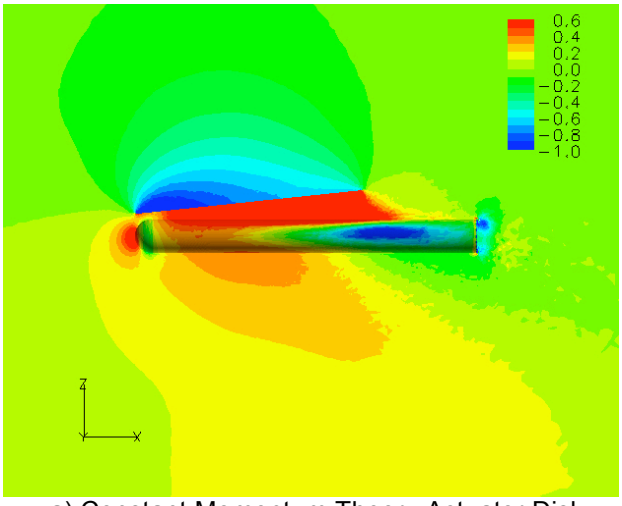

a) Constant Momentum Theory Actuator Disk

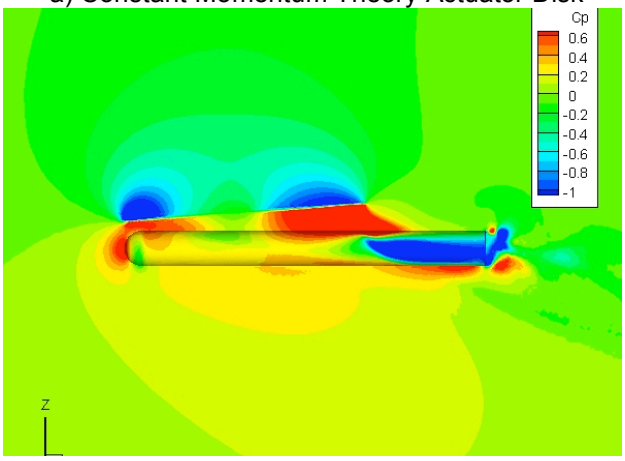

b) Blade element actuator disk

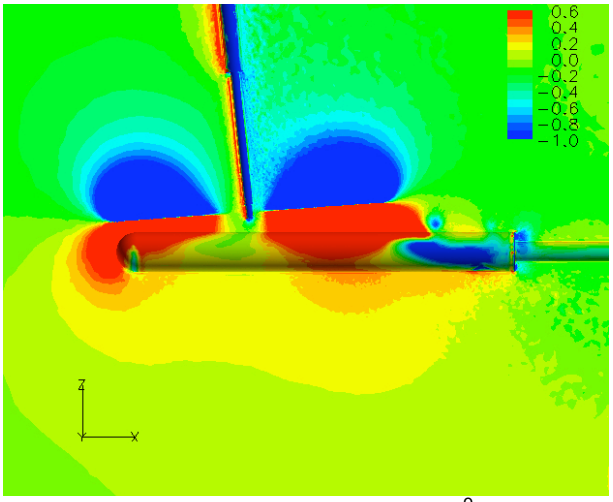

c) Actuator Blades at ψ=0^o

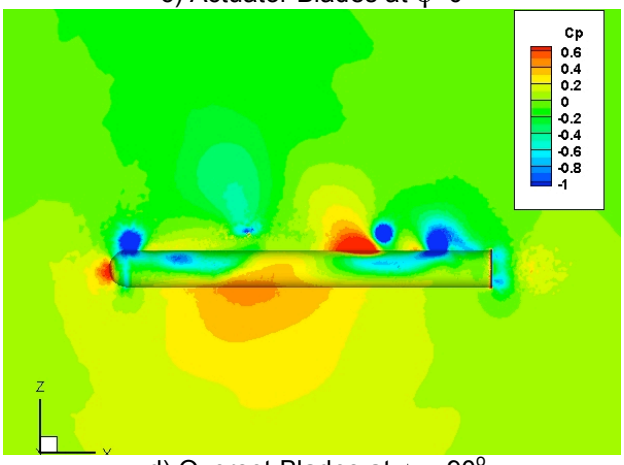

d) Overset Blades at ψ = 90^o

Fig. 6 Pressure coefficient contours on the fuselage surface and for the center line of the flow field

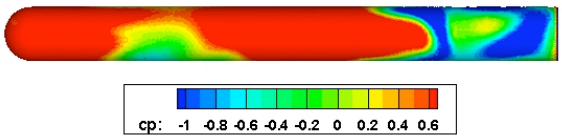

a) Overset Blades at $\psi = 0^o$

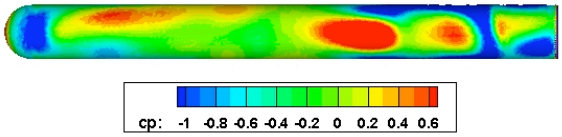

b) Overset Blades at $\psi = 90^o$

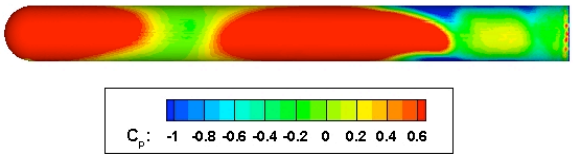

c) Actuating Blades at $\psi = 0^o$

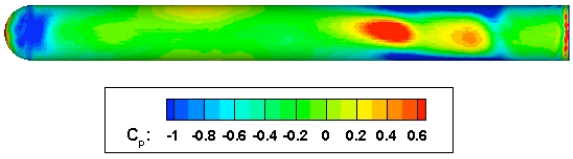

d) Actuating Blades at $\psi = 90^o$

Fig. 7 Pressure coefficients for the unsteady blade models

the wake vortices in the actuating blade model have diffused much faster than the wake vortices in the overset blade model.

Time-averaged Fuselage Pressures

While the unsteady flow field physics are important, the time averaged pressures on the fuselage will indicate how well the simulations have performed over the entire revolution. Here, experimental data is available from Ref. 16 for comparison. The overset blade simulation includes only the first two revolutions, which has potentially degraded the accuracy over the aft end of the fuselage, however the current results indicate that the trends are correctly captured.

For the upper centerline comparison in Fig. 8a, all of the methods except the blade element actuator disk capture the initial suction associated with the acceleration about the hemispherical nose. None of the methods correctly predicts the magnitude of the forward suction peak beneath the rotor, although the overset blades are the most accurate. The constant actuator disk does not differentiate in the pressures across the upper fuselage below the rotor, as was noted in Fig. 6. The remainder of the methods capture the trend of the pressure change, though the overset blade again is most accurate. The blade element actuator disk performs very well in predicting the second peak load, both in magnitude and location. The actuating blades compute the trend of the loading very well, but the peak magnitudes are significantly too low, indicating that the rotor loading is also under predicted.

On the advancing side of the rotor along the fuselage midline, the same double peak pressure loading is observed, though the magnitudes are greatly reduced. Once again the overset blades correlate very well over the first third of the fuselage, but it appears to have not reached its periodic solution over the aft portion of the fuselage. This further indicates the need for additional computational time (more rotor revolutions). The constant momentum actuator disk again does poorly aft of the initial suction at the nose; the midline correlation is much worse than its top centreline correlation. The blade element actuator disk does very well again in comparison with experiment until the last 20% of the fuselage.

On the retreating side of the rotor along the fuselage midline, the time-averaged fuselage pressure distributions continue the trends observed at the other locations. The overset blades track the experimental data very well over the first third of the fuselage again, but misses the location of the second recompression. The overall magnitude of the recompression matches favourably. The simpler rotor models miss the magnitude of the suction area at x/r=0.5 almost completely. On the aft portion of the fuselage, the unsteady actuating blades and blade element actuator disk follow the experiment closer than the other simulations.

Computational Requirements

The different computational requirements are presented in Table 1 for each formulation. All of the runs were computed on an IBM SP3 system with 375 MHz processors. Each processor is configured with 1 GB of RAM. These time/iteration/node figures have been scaled to one processor as the differing rotor models require different numbers of processors. The actuator disk requires the least time per iteration, as expected. The viscous actuator disk requires 22% more time than the inviscid actuator disk when they are run on the same number of

fuselage grid nodes. The preprocessing of the source information is not included in this time estimate. Actuating blades require the most time per node overall, but its grid requirements is comparable to the actuator disk model. Its cost is approximately 2000% greater than a comparable viscous actuator disk. It should be noted that a portion of the increased time requirement is the switch from incompressible to a more stable compressible formulation. Half of the 45% difference in time/iteration/node between the actuator blades and overset blades is cost between the inviscid and viscous formulations. The other half is accounted by the source search algorithm in the actuator blades.

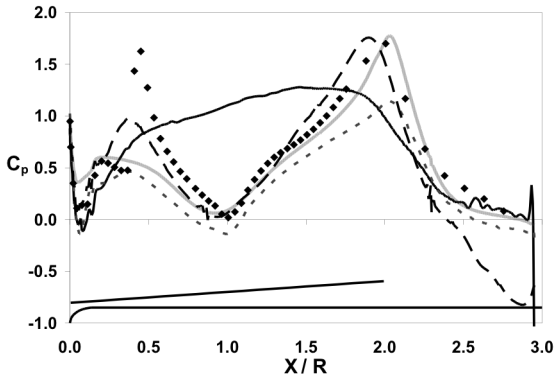

a) Upper Centerline

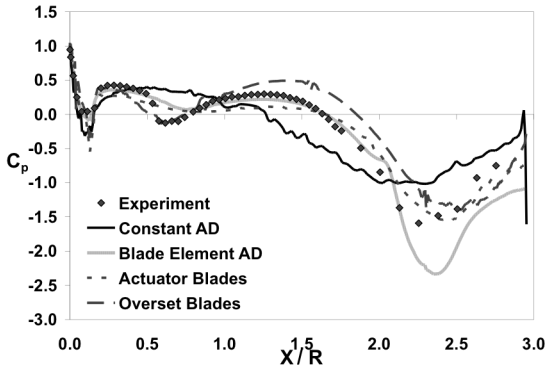

b) Right (Advancing Blade Side)

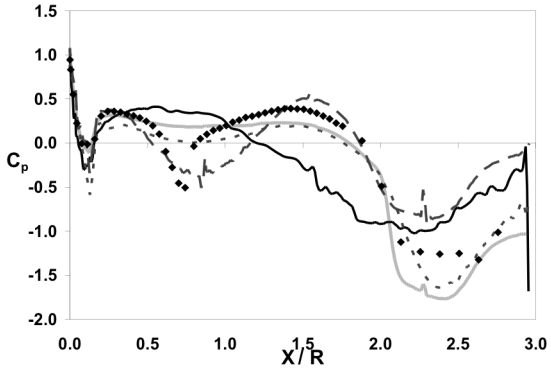

c) Left (Retreating Blade Side)

Fig. 8 Time-averaged fuselage pressure distributions

The time/iteration/node by itself is not the entire computational requirement. The overset grid requires a grid that is 116% larger than the simplified rotor model grids. Thus, a comparison of the clock wall time per iteration indicates that a viscous overset grid (same fuselage grid) requires 1.83 of the viscous actuator blade simulation.

Table 1. Computational Performance Comparison

Rotor Formulation	Time/iteration/ node scaled to 1 processor (μsec)	Grid requirements
Actuator Disk (inviscid, incompressible)	171	1,449,930
Actuator Disk (viscous, incompressible)	210	1,449,930
Actuating Blades(viscous, compressible)	4870	1,449,930
Overset Blades (inviscid, compressible)	3360	3,132,766

Conclusions

Simplified methods of modelling a rotor in conjunction with RANS and Euler fuselage simulations have been analyzed with respect to one another and in comparison with experimental data. The overset blade method, which was known at the outset to be the most physically correct, appears to best capture the unsteady flow field characteristics, as ascertained from rotor theory. Multiple revolutions of the wake vortex structure (two at this time) are captured with little dissipation. On similar grids, the simplified rotor methods are not able to maintain the vortex structure; because of the prediction of lower strength vortices in the rotor near-field, the vortex structure rapidly dissipates. This is important if acoustic and vibration data are needed, indicating the need to perform these expensive computations. Conversely, the actuator disk rotor model, when utilized with blade element theory, can accurately predict the time-averaged rotor loads needed for overall performance computations. These simplified simulations can be completed with approximately 5 – 10% of the computational requirements of the overset blade model. The unsteady actuating blade model holds some promise in predicting the unsteady flow field if the prediction of the rotor loading can be improved. A more efficient nodal search algorithm to decrease its time/node/iteration would also improve the attractiveness of this model.

Acknowledgements

This work is sponsored by the National Rotorcraft Technology Center (NTRC) at the Georgia Institute of Technology. Dr. Yung Yu and Dr. Michael Rutkowski have been the technical monitors of this center. Computational support for the NTRC was provided through the DoD High Performance Computing Centers at ERDC and NAVO through an HPC grant from the US Army, S/AAA Dr. Roger Strawn. The computer resources of the Department of Defense Major Shared Resource Centers (MSRC) are gratefully acknowledged.

References

1. Landgrebe, A., Moffitt, R., and Clark, D., "*Aerodynamic Technology for Advanced Rotorcraft, Parts I and II*," Journal of the American Helicopter Society, Vol. 22, No. 2-3, 1977.

2. Mavris, D., Komerath, N., and McMahon, H., "Prediction of Aerodynamic Rotor-Airframe Interaction in Forward Flight," *Journal of the American Helicopter Society*, pp. 37-46, October 1989.

3. Lorber, P. and Egolf, T.,"An Unsteady Helicopter Rotor-Fuselage Aerodynamic Interaction Analysis," *Journal of the American Helicopter Society*, Vol. 35, No. 3, pp 32-42, 1990.

4. Potsdam, M., Yeo, H., and Johnson, W., "Rotor Airloads Prediction Using Loose Aerodynamic/Structural Coupling," *Proceedings of the American Helicopter Society 60th Annual Forum*, Baltimore, MD, June 2004.

5. Renaud, T., O'Brien, D., Smith, M. and Potsdam, M., "Evaluation Of Isolated Fuselage And Rotor-Fuselage Interaction Using CFD," *Proceedings of the 60th AHS Forum*, Baltimore, MD, June, 2004.

6. Ruffin, S., O'Brien, D., Smith, M., Hariharan, N., Lee, J., and Sankar, L., "Comparison of Rotor-Airframe Interaction Utilizing Overset and Unstructured Grid Techniques," AIAA 2004-0046, AIAA 42nd Aerospace Sciences Meeting, Reno, NV, January 2004.

7. Park, Y. and Kwon, O., "Simulation of Unsteady Rotor Flow Fields Using Unstructured Sliding Meshes," *Proceedings of the American Helicopter Society 58th Annual Forum*, Montreal, Canada, June 2002.

8. Park, Y., Nam, H., and Kwon, O., "Simulation of Unsteady Rotor-Fuselage Interactions Using Unstructured Adaptive Meshes," *Proceedings of the American Helicopter Society 59th Annual Forum*, Phoenix, AZ, May 2003.

9. Hariharan, N., *High Order Simulation of Unsteady Compressible Flows Over Interacting Bodies with Overset Grids*, Ph.D. Thesis, School of Aerospace Engineering, Georgia Institute of Technology, Atlanta, GA, 1995.

10. Chaffin, M. and Berry, J.,"Navier-Stokes Simulation of a Rotor Using a Distributed Pressure Disk Method," *Proceedings of the American Helicopter Society 51st Annual Forum*, Fort Worth, TX, May 1995.

11. Fejtek, I. and Roberts, L., "Navier-Stokes Computation of Wing/Rotor Interaction for a Tilt Rotor in Hover," *AIAA Journal*, Vol. 30, No. 11, Nov. 1992.

12. O'Brien, D. M. and Smith, M. J., "Improvements in the Computational Modeling of Rotor/Fuselage Interaction Using Unstructured Grids," *Proceedings of the 61st Annual Forum of the American Helicopter Society*, June 1-3, 2005.

13. Boyd, D., *Rotor/Fuselage Unsteady Interactional Aerodynamics: A New Computational Model*, Ph.D. Dissertation, Virginia Tech, 1999.

14. Tadghighi, H., "Simulation Of Rotor-Body Interactional Aerodynamics: An Unsteady Rotor Source Distributed Disk Model," *Proceedings of the American Helicopter Society 57th Annual Forum*, Washington, DC, May 2001.

15. Tadghighi, H., and Anand, V., "Simulation of Rotor-Body Interactional Aerodynamics: A Time Accurate Rotor Model ," *Proceedings of the 61st Annual Forum of the American Helicopter Society*, June 1-3, 2005.

16. Brand, A., *An Experimental Investigation of the Interaction Between a Model Rotor and Airframe in Forward Flight*, Ph.D. Thesis, Georgia Institute of Technology, 1989.

17. Bonhaus, D., *An Upwind Multigrid Method For Solving Viscous Flows On Unstructured Triangular Meshes*, M.S. Thesis, George Washington University, 1993.

18. Anderson, W., Rausch, R., and Bonhaus, D., "Implicit/Multigrid Algorithms for Incompressible Turbulent Flows on Unstructured Grids," J*ournal of Computational Physics*, Vol. 128, No. 2, 1996, pp. 391-408.

19. Biedron, R., Vatsa, V., and Atkins, H., "Simulation of Unsteady Flows Using an Unstructured Navier-Stokes Solver on Moving and Stationary Grids," 23rd AIAA Applied Aerodynamics Conference, Toronto, Canada, June 2005.

20. Chorin, A., "A Numerical Method for Solving Incompressible Viscous Flow Problems," *Journal of Computational Physics*, Vol. 2, No. 1, 1967, pp. 12-26.

21. Roe, P., "Approximate Riemann Solvers, Parameter Vectors, and Difference Schemes," *Journal of Computational Physics*, Vol. 43, Oct. 1981, pp. 357-371.

22. Spalart, P. and Almaras, S., "A One-Equation Turbulence Model For Aerodynamic Flows," AIAA Paper 92-0439, 1992.

23. O'Brien, D. M. and Smith, M. J., "Analysis of Rotor-Fuselage Interactions Using Various Rotor Models," AIAA 43rd Aerospace Sciences Meeting, Reno, NV, January 2005.

24. Rajagopalan, R. and Lim, C., "Laminar Flow Analysis Of A Rotor In Hover," *Journal of the American Helicopter Society*, Vol. 36, No. 1, 1991, pp 12-23.

25. Le Chuiton, F., "Actuator Disc Modeling for Helicopter Rotors," *Aerospace Science and Technology*, Vol. 8, 2004, pp 285-297.

26. Zori, L., Mathur, S., and Rajagopalan, R., "Three-Dimensional Calculations of Rotor-Airframe Interaction in Forward Flight," *Proceedings of the American Helicopter Society 48th Annual Forum*, Washington, D.C., June 1992.

27. Noack, R., "DiRTlib: A Library to Add an Overset Capability to Your Flow Solver," 17th AIAA Computational Fluid Dynamics Conference, Toronto, Canada, June 2005.

28. Noack, R., "SUGGAR: A General Capability for Moving Body Overset Grid Assembly," 17th AIAA Computational Fluid Dynamics Conference, Toronto, Canada, June 2005